# Exploration of the Versatile Electrically Augmented Turbine Engine Gearbox Concept

Jonathan L. Kratz[1] and Dennis E. Culley[2]
*NASA Glenn Research Center, Cleveland, Ohio, 44135, U.S.A.*

**Integration of electric machines with the shafts of gas turbine engines is implied in various electrified aircraft propulsion concepts. This includes implementation of the Turbine Electrified Energy Management (TEEM) concept, a motivator for the Versatile Electrically Augmented Turbine Engine (VEATE) gearbox. The VEATE gearbox is a mechanical power transmission concept that seeks to interface electric machines with a gas turbine engine in a synergistic manner. It enables a hybrid electro-mechanical approach for managing power in a gas turbine engine. It is hypothesized that the mechanical design of the VEATE gearbox could be leveraged to enhance the versatility of the present electrical hardware. The VEATE gearbox concept is first introduced and applied to an electrified two-spool advanced geared turbofan meant for powering a single-aisle commercial aircraft. A modeling approach for the gearbox is presented and studies are conducted to investigate the potential application to TEEM and power extraction. There is evidence that the VEATE gearbox could help to reduce the size of the TEEM power system, provide flexibility in power extraction implementation, and exhibit fail-safe design attributes.**

## Nomenclature

<u>English Variables</u>

| | | |
|---|---|---|
| $f$ | = | gearbox force, $lb_f$ |
| $J$ | = | moment of inertia, slug-$ft^2$ |
| $M$ | = | gearbox mass, $lb_m$ |
| $m$ | = | mass of a single planet gear, slug |
| $N$ | = | rotational speed, rpm |
| $n$ | = | number of planets in a planetary gearbox |
| $PR$ | = | pressure ratio |
| $R$ | = | clutch effective radius, ft |
| $SM$ | = | stall margin, % |
| $r$ | = | gear radius, ft |
| $W_c$ | = | corrected flow, $lb_m$/s |

<u>Greek Variables</u>

| | | |
|---|---|---|
| $\Delta t$ | = | simulation time step, s |
| $\eta$ | = | component efficiency |
| $\mu_k$ | = | kinetic coefficient of friction |
| $\mu_s$ | = | static coefficient of friction |
| $\tau$ | = | torque, ft-$lb_f$ |
| $\omega$ | = | rotational speed, rad/s |

[1] Research Engineer, Intelligent Control & Autonomy Branch, Senior AIAA member.
[2] Research Engineer, Intelligent Control & Autonomy Branch, Senior AIAA member.

Subscripts

| | | |
|---|---|---|
| *CA* | = | the variable corresponds to clutch A |
| *CB* | = | the variable corresponds to clutch B |
| *CC* | = | the variable corresponds to clutch C |
| *cg* | = | the variable corresponds to the gear on the carrier that interfaces with electric machine 2 |
| *em1* | = | the variable corresponds to electric machine 1 |
| *em2* | = | the variable corresponds to electric machine 2 or its interface with the carrier/LPS |
| *em2g* | = | the variable corresponds to the gear that interfaces electric machine 2 with that carrier with clutch B |
| *em3* | = | the variable corresponds to electric machine 3 or its interface with the ring gear |
| *em3g* | = | the variable corresponds to the gear that interfaces electric machine 3 with the ring gear with clutch C |
| *hps* | = | the variable corresponds to the high pressure spool or its interface with the speed reduction gear |
| *lps* | = | the variable corresponds to the low pressure spool |
| *p* | = | the variable corresponds to the gearbox planets |
| *pc* | = | the variable corresponds to the interface of the planets and carrier |
| *pr* | = | the variable corresponds to the gear interface of the planets and ring gear |
| *red* | = | the variable corresponds to the gear reduction shaft or its interface with the sun gear |
| *red1* | = | the variable corresponds to the gear on the reduction shaft that interfaces with the HPS |
| *red2* | = | the variable corresponds to the gear on the reduction shaft that interfaces with the sun gear |
| *reds* | = | the variable corresponds to the gear connected to the sun gear that interfaces with the reduction shaft |
| *r* | = | the variable corresponds to the ring gear |
| *rg* | = | the variable corresponds to the gear on the ring gear that interfaces with the gear connected to EM3 |
| *s* | = | the variable corresponds to the sun gear |
| *sp* | = | the variable corresponds to the sun gear and planets |

Acronyms and Abbreviations

| | | |
|---|---|---|
| AC | = | Alternating Current |
| AGB | = | Auxiliary Gearbox |
| AGTF30 | = | Advanced Geared Turbofan 30,000 $lb_f$ – engine model used in the simulation studies |
| APU | = | Auxiliary Power Unit |
| DC | = | Direct Current |
| EAP | = | Electrified Aircraft Propulsion |
| EM | = | Electric Machine |
| EM1 | = | Electric Machine 1 – connected most directly to the sun gear |
| EM2 | = | Electric Machine 2 – connected most directly to the carrier |
| EM3 | = | Electric Machine 3 – connected most directly to the ring gear |
| EOM | = | Equations of Motion |
| GB | = | Gearbox |
| HPC | = | High Pressure Compressor |
| HPS | = | High Pressure Spool |
| LPC | = | Low Pressure Compressor |
| LPS | = | Low Pressure Spool |
| PEx | = | Power Extraction |
| SLS | = | Sea Level Static |
| SP | = | Single Planetary – refers to a VEATE gearbox variant with a single planetary gearbox in the design |
| STARC-ABL | = | Single-aisle Turboelectric AiRCraft with Aft Boundary Layer propulsor |
| T-MATS | = | Toolbox for Modeling and Analysis of Thermodynamic Systems |
| TEEM | = | Turbine Electrified Energy Management |
| VEATE | = | Versatile Electrically Augmented Turbine Engine (VEATE) |

## I. Introduction

Electrified aircraft propulsion (EAP) systems are being investigated to address the challenge of reducing fuel burn, emissions, and noise [1]. This applies to all classes of commercial air vehicles ranging from air taxis for urban air mobility [2] to single-aisle and larger transports. NASA has proposed several EAP concepts including the Single-aisle Turboelectric AiRCraft with Aft Boundary Layer propulsor (STARC-ABL) [3] and N3-X [4]. Many of these concepts include electrified turbomachinery in which electric machines (EMs) are mechanically coupled with the spools of gas turbine engines for power extraction (PEx) and or power injection. While some concepts only consider power extraction or injection on a single spool of a multi-spool gas turbine engine, studies have been conducted showing optimal power splits that utilize EMs on both spools of a two-spool engine [5]. The term 'power split' refers to the fractional split in the engine power extraction between the High Pressure Spool (HPS) and Low Pressure Spool (LPS). Furthermore, there are applications for EMs on both spools of a gas turbine engine that include engine starting and power/energy management control strategies such as Turbine Electrified Energy Management (TEEM) [6]. Therefore, it is expected that advanced aero-propulsion concepts will include electric machines integrated with multiple spools of a turbofan or turboshaft engine.

There is also a trend for more electrified engines that can include the addition or increase in power level of electric machines and energy storage devices that are integrated with the engines. The electric machines can be used for a variety of purposes such as for turbine electrified energy management (TEEM) [6,7,8]. TEEM seeks to leverage electric components, mainly electric machines and energy storage elements, to improve the operability of the turbomachinery. Consequently, the improved control over engine operability enables new capabilities for the propulsion system and the aircraft it propels. Operability benefits can be leveraged in the engine design process to improve system safety, weight, and or performance. Ref. [9] outlines some of the operability considerations that impact turbomachinery design. In particular, Ref. [9] points out that the engine design process is "a complex compromise between efficiency targets, number of stages, surge margin requirements across the intended flight envelope, and various mechanical considerations, such as stress limits, vibration, etc.". It goes on to explain that it is important for the compressors to have sufficient working surge margin that will ensure stable operation of the engine throughout the flight envelope for all likely transient conditions. Required surge margin is determined empirically and Ref. [9] attributes it to 3 main factors that contribute roughly equally. One of those factors is a shift in the operating line during transients. Often times, the maximum efficiency of the compressor is achieved closer to the stall line and the shift in the operating line to appease operability constraints may cost several percentage points in compressor efficiency. The operability constraint will force a compressor to operate at a less efficient operating point on the map and/or be designed less aggressively to achieve a lower maximum efficiency. Either way, compressor efficiency is sacrificed, and that ultimately leads to sacrifices in overall performance metrics such as fuel burn. It has been shown through simulations in Ref. [6,7,8], that substantial transient operability benefits can be obtained with relatively modest electric machine power levels and energy storage capacity. This could alleviate the need for design constraints, and thus enable more efficient turbomachinery. TEEM may provide various other benefits, but for the purpose of this study the focus will remain on the transient operability application of TEEM.

There are numerous possibilities for how the integration of the EMs with turbomachinery could be achieved. The Versatile Electrically Augmented Turbine Engine (VEATE) gearbox is a potential approach. The VEATE gearbox is a mechanical transmission that consists primarily of gears, shafts, and clutches. The design consists of at least one gearbox that operates in a manner similar to a planetary gearbox. That is, it has 3 coupled rotating components similar to the sun gear, carrier, and ring gear of a planetary gearbox. Variations of a basic planetary gearbox, such as the Offset Compound Gearbox and Dual Star Idler Gearbox designs described in Ref. [10], may also be used in place of a conventional planetary gearbox. In this study, a conventional planetary gearbox design is assumed. The different components of the planetary system could be connected to an engine spool, an electric machine, a component of another planetary gearbox, or a component that interfaces with one of these parts. Clutches may exist to modify the configuration of the mechanical transmission to influence the path of power flow and to isolate faults when they occur.

A particular version of the VEATE gearbox is investigated in this paper. This version has a single planetary gearbox in its design and will be referred to as the Single Planetary (SP) variant. Figure 1 illustrates the basic planetary gearbox anatomy. Planetary gearboxes are used in a variety of applications, including automotive power transmissions, conveyers, robots, pencil sharpeners, etc. They have applications in many industries including aerospace. Planetary gears have a much higher contact ratio than spur gears, which provides significantly more torque capacity, among other benefits. Typically, they

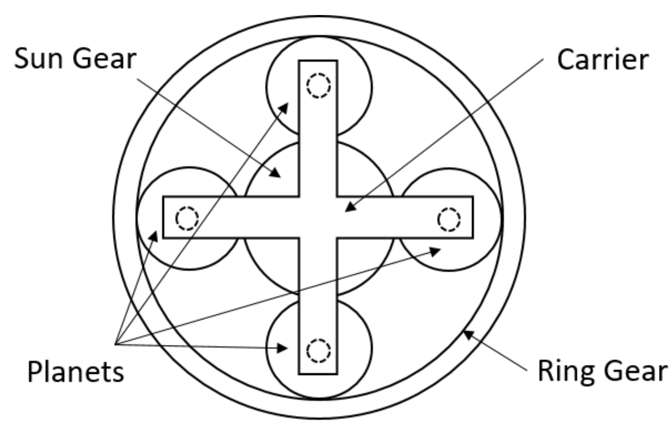


**Figure 1. Simple planetary gearbox schematic**

are used to change the speed between two rotating components such that one is at high speed and low torque while the other is at low speed and high torque, thus allowing each component to operate within their desired speed range. It is common for one of the three main components (sun gear, ring gear, and carrier) to be held stationary while the other two components function as input and output. The dimensions of the gearbox components determine the speed and torque ratios at the interfaces. Gear ratios for a single planetary gearbox with a stationary component, typically range from 3:1 to 10:1. In the application investigated in this paper, all of the gearbox components will be able to move. The ability to influence the speed of the components, in particular the one that is normally stationary, provides the ability to manipulate the speed ratio as well as to manage power in the system.

The purpose of this paper is to introduce a simple form of the VEATE gearbox, present a model for capturing its behavior, and investigate the impact that the gearbox could have on the propulsion system. In particular, the applications of interest include transient operability control through TEEM, large scale power extraction, and reversionary control usages relevant to those two applications. While this paper will not be able to address these potential applications in detail, the studies are sufficient to demonstrate potential for the concept. Also note that the physical characteristics of the VEATE were not optimized but were selected based on engineering judgement and are thought to be a decent starting point that is sufficient to fulfill the purposes of this paper. Throughout the simulation studies, comparison will be referenced to a baseline turbofan engine model. It will also be compared with a modified version of the engine model configured with what will be referred to as a Dedicated EM (DEM) approach. In the DEM approach, each spool has its own dedicated EM and gearbox. The EMs are only able to directly affect the spool to which they are interfaced.

The remainder of this paper is organized as follows. Section II provides background about the applications of TEEM and large-scale power extraction. Section III describes the Advanced Geared Turbofan 30,000 $lb_f$ (AGTF30) engine model that is utilized as an application testbed for this study. Section IV provides a more detailed description of the VEATE gearbox concept. Section V presents modeling of the VEATE gearbox and its integration with the AGTF30 engine model. Section VI discusses simulation studies and Section VII presents a mass analysis. Finally, Section VIII provides concluding remarks. Appendix A and Appendix B provide details of the VEATE gearbox model. Appendix A includes relevant equations and a detailed description of the solution procedure. Appendix B provides the parameters utilized by the model.

## II. Background on TEEM and Large-Scale Power Extraction

The two applications of the VEATE gearbox explored in this paper are with respect to large-scale power extraction and TEEM. To provide a basis for comparison, these applications are discussed in the context of how they would be applied with a DEM approach. For large-scale power extraction, various EAP concepts consider large amounts of power extraction from the LPS compared to the HPS. For example, STARC-ABL [3], pictured in Fig. 2, extracts nearly 2000 hp from each of its underwing engines to drive an aft boundary layer ingesting tail fan. All that power is extracted from the LPS while only 350 hp is extracted from the HPS for other aircraft system power demands. This split in power would force the LPS EM to be very large or it would require interfacing multiple EMs to the same shaft. The relatively large amount of power extraction from a single spool may complicate EM and engine integration. Furthermore, a LPS EM failure would result in a loss of all power from that engine going to the tail fan. Concepts like STARC-ABL benefit from accelerating the low momentum boundary layer to reduce profile drag while creating thrust, thus the loss of power to the tail fan causes even more significant loss of net thrust. For these reasons, flexibility in the power extraction implementation that allows for more even power splits between the EMs could be advantageous.

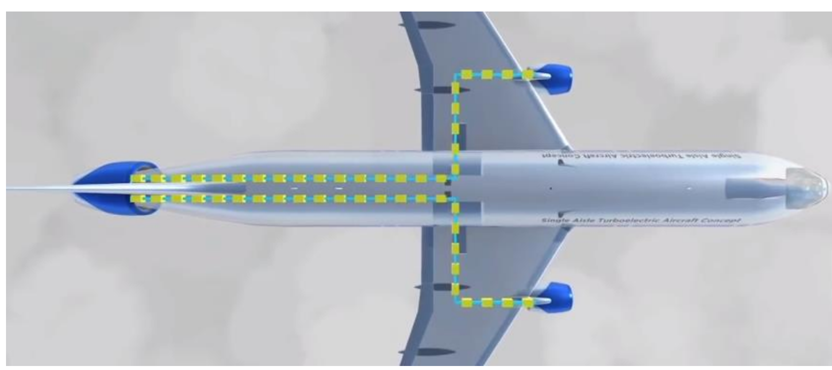

**Figure 2. A rendering of the STARC-ABL concept. The wing mounted geared turbofans supply power to drive the tail fan.**

TEEM leverages the electrical power system integrated with turbomachinery to improve transient engine operability. Primarily it seeks to improve compressor operability. During a transient, the fuel flow rate is changed to

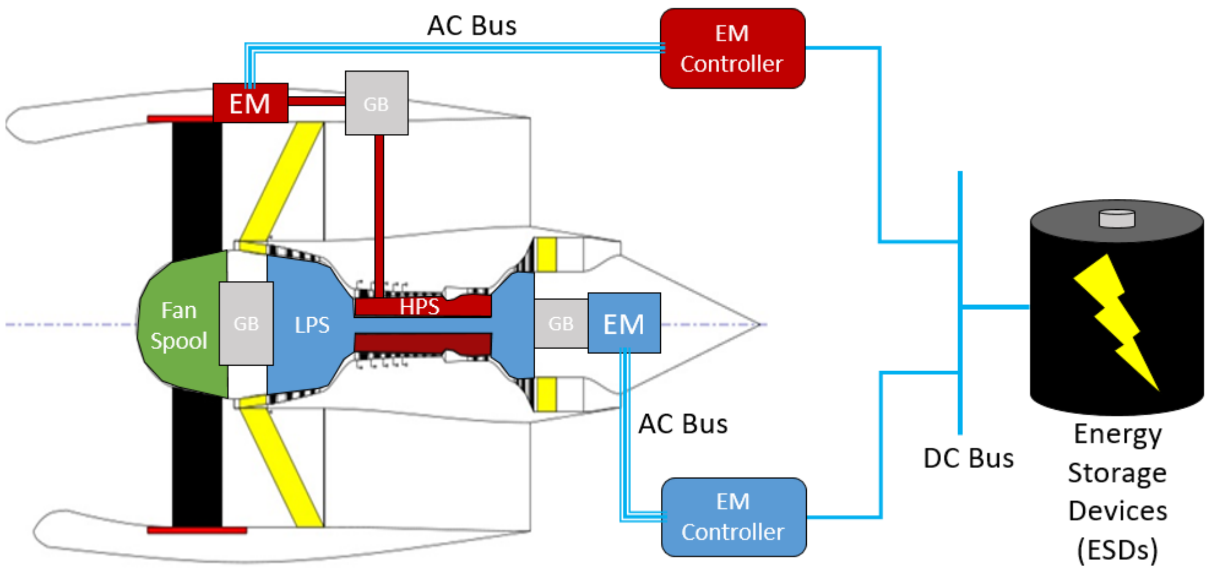


**Figure 3. The DEM system for applying TEEM. AC and DC stand for alternating current and direct current respectively**

modify the flow condition inside the engine. However, the speeds of the spools do not change instantaneously due to their large inertias. This creates a mismatch between the flow condition and rotational blade speed that results in off-incidence flow and may stall the compressor if it becomes severe enough. Typically, the HPC tends to move closer toward stall during acceleration transients while the LPC tends to move toward stall during decelerations. Having the ability to influence the shaft speeds with electric torque independent of the fuel flow rate allows the EMs to overcome much of the inertia of the engine spools to operate closer to steady-state design conditions while a transient is occurring. This keeps the compressor blades from experiencing severe off-incidence angles relative to the air moving through the engine. The ability to tightly maintain blade incidence angle improves operability and enables new possibilities for the engine design.

The system pictured in Fig. 3 is representative of the DEM approach for TEEM. Each spool has a dedicated EM that is connected to its respective shaft through its own gearbox (GB). The EMs are managed by their respective power controllers that are connected to a common power bus. An energy storage system, which may consist of numerous energy storage device (ESDs), is present on the DC bus and supplies or absorbs power in response to the operation of the EMs. References [7] and [8] demonstrate the application of TEEM with such a system.

Figure 4 illustrates the basic concept of how the EMs are used to improve operability during transients. The control approach described in Ref. [7] utilizes the HPS EM to apply power to the HPS during accelerations in order to improve the transient operability issues. It was found that the use of the LPS EM to assist was not effective. The need to inject power with the HPS EM tends to drive the energy storage system requirements. During decelerations, the LPS EM can be used to extract power from the LPS and or the HPS EM can apply power to the HPS to improve operability. A good strategy is to extract power with the LPS EM and apply that power with the HPS EM [8]. This will prevent any issues with managing excess power while simultaneously addressing the operability issues. In addition, this enables the LPS EM to be reduced in size. A closed loop control strategy is implemented with relevant details provided in Ref. [7] and [8]. The HPS EM controller attempts to maintain the steady-state HPS speed vs. fuel flow relationship throughout acceleration transients. During deceleration transients, the LPS EM controller attempts to maintain the steady-state LPS speed vs. fuel flow relationship and the HPS EM is commanded to apply power to the HPS equivalent to the amount of power commanded to be extracted from the LPS.

Figure 5 shows results for the DEM implementation of TEEM for a sea level static (SLS) burst and chop transient in which the throttle is quickly moved from idle to maximum power and then quickly moved back to idle.

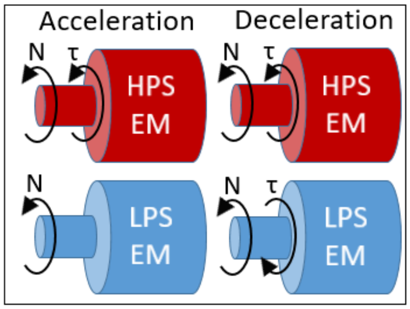


**Figure 4. Basic uses of EMs during transients to implement TEEM**

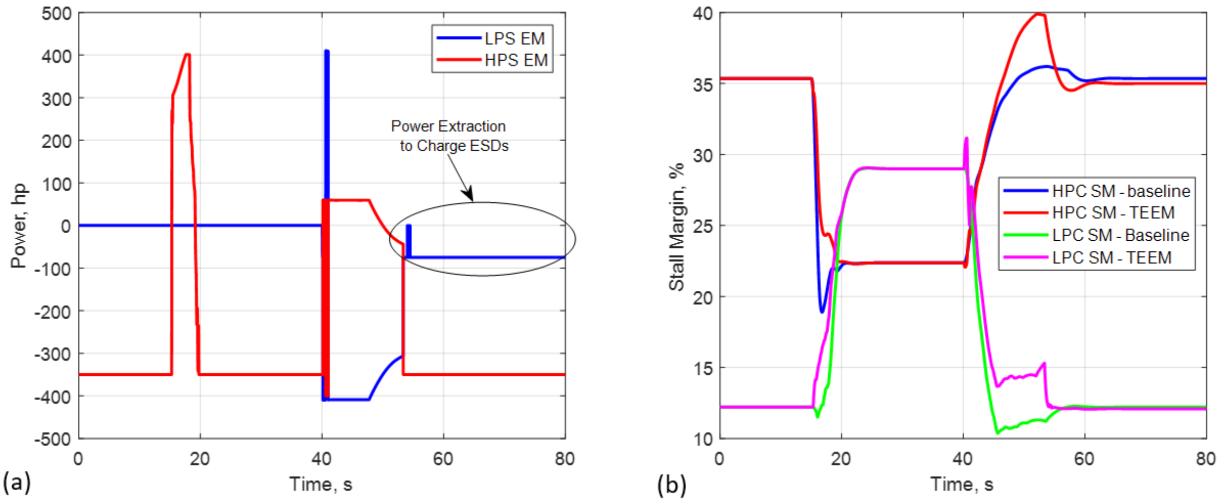


**Figure 5. Example results for the DEM approach as applied to TEEM. (a) Shows the EM power inputs and (b) shows the HPC and LPC stall margins compared with a baseline simulation in which TEEM is not applied. The power extraction with LPS EM circled in (a) is for re-charging the ESDs.**

Fig. 5a shows the power inputs on the engine spools and Fig. 5b shows the impact on the HPC SM and LPC SM compared to the baseline response without TEEM. The improvement in HPC and LPC operability is evident by the elevated minimum stall margin during the transients.

There are a few short comings associated with the DEM implementation of TEEM. One is that, for applications like the AGTF30, the LPS is not effective at aiding the HPS during accelerations and therefore it is underutilized. If other EMs were able to aid the HPS EM, HPC operability could be further improved to promote safety or it could enable the HPS EM to be smaller and lighter. Also, in the event of an HPS EM failure, there would be no effective way to maintain the operability benefits promised by TEEM during acceleration transients. This can be important because, in theory, operability margin would be removed from the engine to achieve better efficiency and or a lighter weight engine. Without the ability to use the electrical power system to protect against stall, the engine would either be forced to operate with uncomfortably degraded operability or it would be forced to accept a more sluggish thrust response. Both options are undesirable, especially if a better option existed. Note that TEEM may be implemented together with large scale power extraction.

## III. The AGTF30 Model

The AGTF30 is a dynamic model of a conceptual advanced geared turbofan engine [11]. The engine is capable of producing ~30,000 $lb_f$ of thrust at SLS conditions. It features a compact core and variable area fan nozzle (VAFN). The AGTF30 engine is modeled with the Toolbox for Modeling and Analysis of Thermodynamic Systems (T-MATS) [12], which leverages MATLAB/Simulink™. It was created to match the performance of the NASA N+3 reference engine that was originally modeled in Numerical Propulsion System Simulation (NPSS) code [13]. The engine model incorporates shaft dynamics and is accompanied by a realistically performing controller with limit logic [14] that exhibits representative dynamic behavior. Figure 6 is a schematic of the engine cross-section that was produced with NPSS WATE++ code [15]. The baseline AGTF30 is a two-spool gas turbine engine with a geared fan. There are no electric machines, no energy storage devices, and no mechanical coupling between the LPS and HPS. A total of 350 hp is extracted from the HPS through an auxiliary gearbox (AGB) for the purpose of powering aircraft systems. For the purpose of this paper, the engine model has been modified to include

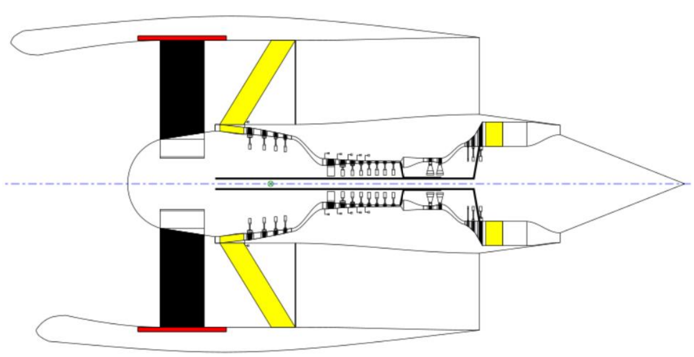

**Figure 6. AGTF30 cross-section schematic**

the VEATE gearbox model described in Section V, which also enables supplemental torques to be applied to the engine spools using multiple EMs.

## IV. Description of the VEATE Gearbox Concept

The VEATE gearbox is an electro-mechanical system for managing power in a gas turbine engine. It uses EMs to apply and or extract power as well as transfer power mechanically by leveraging the components of the gearbox system, including the engine spools. Clutches may be used to modify the path of power transfer or to isolate failures such as an EM with a locked rotor.

A VEATE gearbox concept seeks to interface one or more electric machines with the spool(s) of a gas turbine engine through a gearbox. The overall system may consist of one or more gearboxes that each operate like a planetary gearbox where torque applied to the sun gear, the ring gear, or the carrier, impacts the speed of all 3 components. Alternatives to mechanical gearing may be possible, but for demonstration purposes traditional mechanical planetary gearboxes are assumed throughout the rest of this description and the studies that follow. The components of the planetary gears may be connected to a spool of the gas turbine engine, an electric machine, a component of another planetary gearbox, or a component that interfaces with any of these parts. The connections may be direct or they may occur through a clutch. The type of gearing and clutches are not prescribed. There can obviously be many variants of a VEATE gearbox.

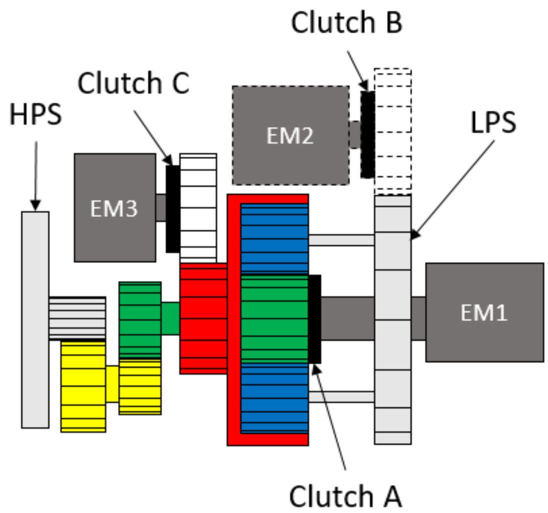


**Figure 7. Schematic of the VEATE gearbox SP variant**

The focus of this study is on the simplest form of the VEATE gearbox, which is the SP variant. Figure 7 shows a basic representation of the SP gearbox. It is comprised of a single planetary gearbox whose main components are the sun gear (green), planets (blue), ring gear (red), and carrier (light gray). In this configuration, the carrier is directly connected to the LPS and the sun gear is rigidly connected to the HPS through a speed reduction gear (yellow). The EMs and their shafts are colored dark gray. They are identified as EM1, EM2, and EM3. The clutches are identified as Clutch A, Clutch B, and Clutch C. They can be independently used to connect/disconnect EM1, EM2, and EM3 to the rest of the system. These clutches are envisioned to be engaged under normal operation and only disengaged in the event of EM failures. EM2, Clutch B, and its interface gear are outlined with dashed lines in Fig 7 because these components will be present in some of the applications, but not in others.

The primary role of EM1 and EM2 is to influence the speeds of the engine spools, thus impacting the operability and performance of the engine. EM1 will primarily be used to impact the HPS, while EM2 is used to primarily impact the LPS. EM3 creates a mechanical coupling effect between the spools. EM3 can be used to provide leverage between the HPS and LPS. It has the capability to influence both the transfer of power between them, as well as their speed ratio, while simultaneously adding or extracting power to/from the overall system. The SP gearbox has 8 possible configurations, which result from all of the possible combinations of clutch engagements. However, for the applications of this study, the clutches should always be engaged during normal operation. The rigid mechanical power flow paths are highlighted by different colors in Fig. 8 with all clutches engaged. The term 'rigid mechanical power flow path' refers to a mechanical path through which power can be transferred effectively due to the rigid coupling of the components. For example, EM1, the speed reduction shaft, and the HPS make a rigid power flow

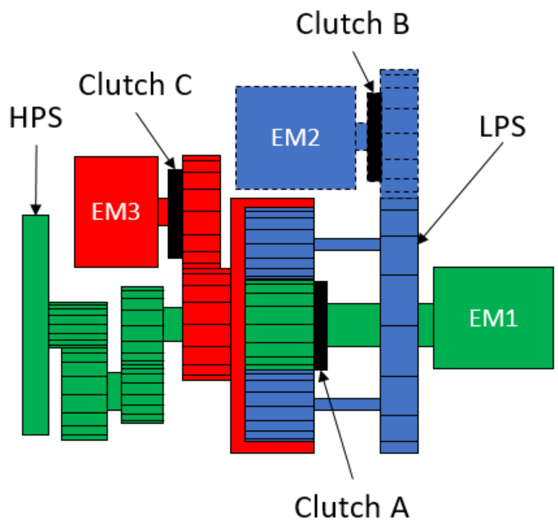


**Figure 8. Rigid power flow paths for the SP gearbox with all clutches engaged**

path because power can be effectively transferred between them without outside influence. In contrast, EM2 is not connected to the HPS through a rigid power flow path because without the effort of EM3, the ring gear lacks the rigidity necessary to transfer power between these components.

## V. The VEATE Gearbox Model

The dynamic VEATE gearbox model captures the motion of the gearbox components (gears, carrier, and shafts), the electric machines, and the engine spools. The model description presented here is specific to the SP variant. Nomenclature for the various model parameters is introduced first. The radii of the gears are generally expressed with the variable, $r$, and an identifiable subscript. These variables are defined in Fig. 9. Including the 3 EMs and 2 engine spools, the SP gearbox model consists of 11 components (only includes 1 of the planets) with distinct operating speeds. Each of the components have a moment of inertia denoted by, $J$, and an efficiency, $\eta$, that attempts to account for losses. These parameters are appended with the identifiable subscripts listed in Table 1. The planet gears have two unique parameters: the number of planet gears, $n_p$, and the mass of each planet gear, $m_p$. While no specific type of clutch is assumed in the VEATE gearbox, clutches are modeled here as friction clutches for simple demonstration. Each clutch has an associated effective radius $R$, normal force $X$, kinetic coefficient of friction $\mu_k$, and static coefficient of friction $\mu_s$. Each variable is appended by a subscript of $CA$, $CB$, or $CC$, to clarify which clutch it corresponds to. Torques are denoted with $\tau$. Input torques from the HPS, LPS, and EMs utilize subscripts listed in Table 1. Torques created by the clutches use the clutch subscripts ($CA$, $CB$, and $CC$). The speed of each component in rpm is denoted with $N$ followed by the respective component subscript identifier. When the speed is expressed in units of rad/s, $\omega$ is used. The angular acceleration is expressed with $\dot{\omega}$. Forces at the gear interfaces use the variable $f$. Figure 10 shows the location of the seven gear forces and defines the variables for each. Positive forces are defined to go into the page. Note that forces are only marked at unique interfaces. The forces associated with the planets ($f_{sp}$, $f_{pr}$, and $f_{pc}$) can be multiplied by a factor of $n_p$ to get the overall force between the planets and the relevant component.

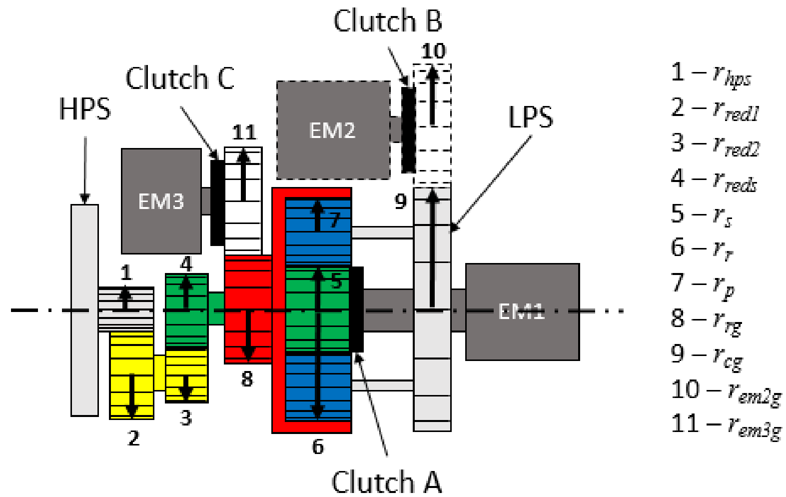


**Figure 9. Definition of radii variables**

**Table 1. VEATE gearbox model component subscript identifiers**

| Component | Subscript Identifier |
|---|---|
| High pressure spool | *hps* |
| Low pressure spool (same as the carrier) | *lps* |
| Speed reduction shaft | *red* |
| Sun gear | *s* |
| Planets | *p* |
| EM1 + shaft | *em1* |
| EM2 + shaft | *em2* |
| EM3 + shaft | *em3* |
| EM2 gear | *em2g* |
| EM3 gear | *em3g* |

There are seven "base" equations of motion (EOMs) that govern the dynamics of the 11 gearbox components. The seven equations ensure the motion predicted by the model does not violate the constraints placed upon it through the physical coupling of the gearbox components. Specifically, the velocity of the gears at the gear interfaces must match. Furthermore, the angular acceleration of the carrier components must satisfy expressions derived from a torque balance on the carrier, and a force balance on the planets. The first six of the seven equations require the velocity of the gearbox components at their interfaces to match. The last equation reconciles expressions for the LPS/carrier dynamics (more on this later). The seven equations are provided below.

$$r_{hps}\dot{\omega}_{hps} = -r_{red1}\dot{\omega}_{red} \tag{1}$$

$$r_{red2}\dot{\omega}_{red} = -r_{reds}\dot{\omega}_s \quad (2)$$

$$r_s\dot{\omega}_{lps} - r_p\dot{\omega}_p = r_s\dot{\omega}_s \quad (3)$$

$$r_r\dot{\omega}_{lps} + r_p\dot{\omega}_p = r_r\dot{\omega}_r \quad (4)$$

$$r_{cg}\dot{\omega}_{lps} = -r_{em2g}\dot{\omega}_{em2g} \quad (5)$$

$$r_{rg}\dot{\omega}_r = -r_{em3g}\dot{\omega}_{em3} \quad (6)$$

$$\dot{\omega}_{lps} = \dot{\omega}_{lps} \quad (7)$$

Expressions for the angular accelerations come from the dynamic equations of each component and are derived from a force and torque balance analysis. With clutches engaged, multiple components can be coupled. In such a case, dynamic equation(s) are derived from a force and torque balance analysis of the collection of coupled components. Note that directly coupled parts refers to multiple components that spin at the same speed due to their direct connection through a clutch. The equation(s) that describe the new coupled component replaces the equations that defined the dynamics of the uncoupled components. The complete set of equations are provided in Appendix A. Some additional explanation is warranted for Eq.7. The left hand side of Eq. 7 is the result of a torque analysis for the LPS (also the carrier in this configuration), and the right hand side is the result of a force analysis for the planets. To be explicit, Eq. 17 and Eq. 18 in Appendix A form the right and left hand sides of Eq. 7, respectively. The unknowns are the seven gear forces. Eq. (1) - (7) form a set of seven linear equations that can be solved using linear algebra techniques.

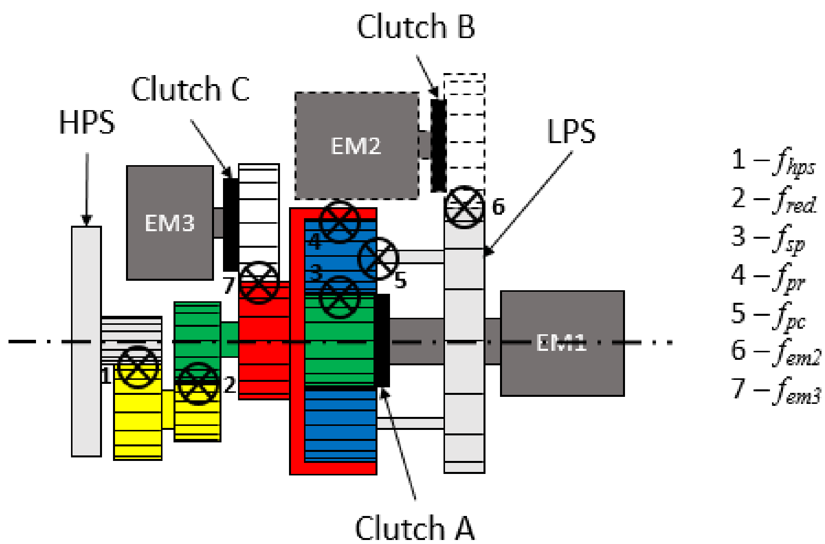


**Figure 10. Definition of gear force variables**

In addition to the seven EOMs listed above, there could be up to three more EOMs, one for each clutch. These EOMs are used during clutch engagement and they seek to match the speeds of the rotating parts on each side of the clutch once the clutch engagement is complete and the rotating parts are “locked”. In this context, the term “locked” refers to a condition where the clutch has achieved the same speed in both components to which it connects, and the two components rotate together as a single component. Without such equations, the rotating parts on each side of a clutch will have difficulty matching speeds precisely at the end of a discrete time-step, particularly if the time-step and or the clutch torque applied during the “lock-up period” is relatively large. Depending on how the clutch lock-up is handled in the model, failure to address this issue could prevent the clutch from achieving the same speed on both sides of the clutch. This could cause the clutch model to have issues achieving the desired “locked” condition. This is because the speed of the two components may continually overshoot each other. Another possibility is that the model could settle on a “lock-up condition” where there is a significant speed difference between the two components that should be rotating at the same speed. The additional equations address this issue and are only added to the system of equations during the “lock-up” phase in which a clutch has been commanded to engage and a speed crossing is predicted. Here, a speed crossing refers to the speed of one rotating component crossing over the speed of the component on the other side of the clutch. A first order forward difference approximation is used to predict if there will be a speed crossing during the next time step of the simulation. If a speed crossing is predicted, then the additional equation for the relevant clutch is added to the system of equations and the corresponding clutch torque becomes a new unknown. Essentially this means solving for the clutch torque that will result in a speed match at the end of the simulation time step. Eq. 8 is a generic version of the new system equation where subscript "a" and "b" refer generically to the components on each side of the clutch.

$$\dot{\omega}_a - \dot{\omega}_b = \frac{1}{\Delta t}[\omega_b(t\text{-}\Delta t) - \omega_a(t\text{-}\Delta t)] \tag{8}$$

For example, consider if clutch A were commanded to engage and a speed crossing was predicted. In this case Eq. (8) would become:

$$\dot{\omega}_s - \dot{\omega}_{em1} = \frac{1}{\Delta t}[\omega_{em1}(t\text{-}\Delta t) - \omega_s(t\text{-}\Delta t)]$$

Once the linear system is solved and all the forces and torques are known, those values can be substituted into the expressions for the time rate of change of rotational speeds. These values are integrated to get the component speeds, which are also used in the next time step of the model.

Some iteration is used within the VEATE gearbox model to ensure that the correct "clutch lock configuration" achieves convergence. Multiple clutches could be simultaneously in a state of engaging. In this case, one or more clutches are in the process of locking up, but are slipping. The commanded clutch configuration could also change during the lock-up period of a clutch. In addition, static friction forces can be exceeded causing unplanned slippage of the clutches. All of these conditions can alter the dynamics of the gearbox and they can impact the clutch lock configuration. The clutch lock configuration can alter the calculation of the clutch torques and the formulation of the EOMs. Hence the need for iteration to ensure the clutch lock configuration converges. The iterative procedure is outlined in Appendix A.

The VEATE gearbox model was implemented as a user-defined Simulink block. This block replaced the T-MATS shaft dynamics blocks for the HPS and LPS within the AGTF30 model. The block accepts various inputs including the torques imparted on the HPS and LPS through the engine flow path, and from torques applied by each of the EMs. Inputs also include the speeds of the shafts, EMs, and each component of the gearbox. The final inputs to the block are the clutch commands (engaged or disengaged). The outputs are the rates of change of speed of each of the engine spools, the mechanical gearbox components, and the electric machines. The block resides within an iterative solver that seeks to satisfy steady-state conservation laws for the working fluid within each of the engine components. Thus, the rates of change in speed are integrated outside of the iterative solver layer of the Simulink model. The component speeds are fed back to the model as inputs for the next iteration. The parameters of the model are provided in Appendix B. Value selection for some of the parameters can have implications on the operation of the VEATE gearbox. For instance, changing the ratio of sun gear and ring gear radii would alter the speed of the ring gear and could even change the direction that it spins. Since the point of this study is to investigate the operational feasibility and general utility of the VEATE gearbox system, no attempt to optimize the selection of model parameters or to perform a parametric study was undertaken. The parameters listed in Appendix B are thought to be a reasonable starting point for the objectives of this study.

## VI. Simulation Studies

The simulation studies are presented in three sub-sections. The study covered in Sub-section A uses the VEATE gearbox model to extract and apply power with the EMs with respect to a nominal power extraction schedule. Observations are made about the impact this action has on the operating point of the compressors and the balance of power between the engine spools. This study identifies trends that are used to direct the other two studies. Sub-section B covers a study that applies the VEATE gearbox to the TEEM control problem. In that study there is no nominal power extraction or injection beyond that required by the aircraft system (350 hp of power extraction from the HPS). The third study, covered in Sub-section C, investigates large scale power extraction and reversionary control strategies are illustrated. In each of these studies the results are compared against the DEM approach. The baseline AGTF30 is used as a reference point in some cases as well.

### A. Basic Power Injection/Extraction Study

In this study, power is extracted and applied with each of the EMs with respect to a nominal power extraction schedule. This action is taken to observe the impact of power extraction on the engine, particularly the LPC and HPC operability. In this case, EM1 nominally extracts 350 hp to meet the aircraft system power demand. Of particular interest is the impact of EM3 due to its indirect interfacing with the engine spools as opposed to EM1 and EM2. The simulation study employed the AGTF30 engine model at sea level static (SLS) conditions. All of the clutches are engaged for this study as illustrated in Fig. 8. The simulations were conducted at 80% of maximum thrust. Off-nominal power of ±500 hp was applied with each EM in different simulations, independent of the other EMs. When an EM was not used, it was allowed to freewheel. A simulation without any off-nominal power injection or extraction was also performed to establish a baseline. In each simulation, the fuel flow rate was adjusted to maintain the same corrected fan speed and the VAFN area was allowed to vary from its schedule to maintain the same fan stall margin (VAFN area changed less than 0.1% of the maximum nozzle area). This strategy keeps the fan operating point the same and achieves essentially the same engine thrust for all test points. Thus, the set of power injection results, and the set of power extraction results can be compared fairly in terms of performance and operability. The simulation study is rather simple, but it provides valuable information pertaining to the applications being considered.

It was observed that when power is added/extracted by EM1, that power is added/extracted almost entirely to/from the HPS. In other words, EM1 acts similar to the HPS EM in the DEM approach and can be considered equivalent and capable of doing everything that the HPS EM can do in the DEM approach. The same claim about EM2 can be made with respect to the LPS EM in the DEM approach. Both of these observations are the result of negligible coupling between the HPS and LPS without the use of EM3. However, Fig. 11 shows what happens when EM3 is used. Applying or extracting power with EM3 creates a coupling effect between the LPS and HPS that influences power transfer between the spools. In this example, ~0.75-0.78 hp is transferred between the spools for every 1 hp that is applied with EM3. Power injection with EM3 causes power to be shifted from the HPS to the LPS and power extraction has the opposite effect.

From prior TEEM studies with the AGTF30 [7,8], it is evident that power addition on the HPS and power extraction on the LPS are beneficial for the HPC and LPC operability during transients. Fig. 11 demonstrates that power extraction with EM3 accomplishes both objectives. Compared to power extraction with EM2 (comparable to the LPS EM in the DEM approach), power extraction with EM3 influences an even greater reduction in power on the LPS and a simultaneous increase in power on the HPS. Thus it is expected that EM3 will be more effective at improving operability during deceleration transients than EM2 (or the LPS EM in the DEM approach). Given its apparent greater effectiveness, it is hypothesized that EM3 could accomplish the same task with less power. EM2 could be removed entirely or omitted from use with TEEM and therefore not be subjected to the off-nominal power requirements imposed by TEEM. In either case, it is believed that the power system size could be reduced. Also, EM3's ability to shift power to the HPS could supplement the work of EM1 (comparable to the HPS EM in the DEM approach) or be used in its place during accelerations. This provides another option for handling acceleration transients in the event that EM1 fails. It also provides a potential opportunity to reduce the size of EM1. Finally, because EM3 extracts power in order to shift power to the HPS, the power extraction with EM3 is expected to help offset the power demand from EM1, and this will reduce the power and energy requirements for the energy storage system.

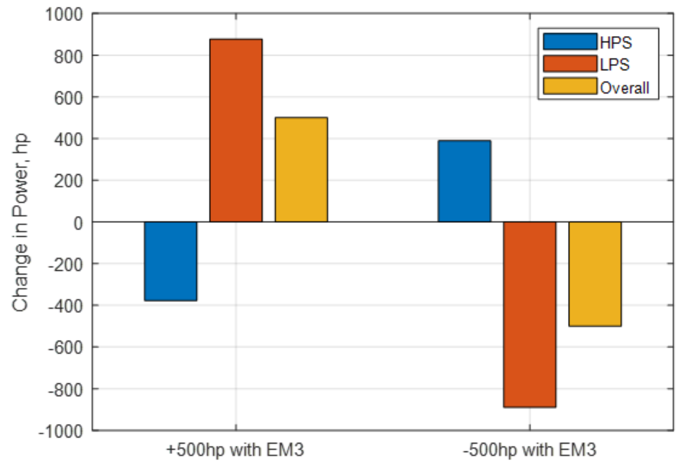


**Figure 11. Impact of EM3 power injection and extraction on the power balance on the engine spools**

The results shown in Fig. 12a and 12b provide more evidence to support the observations and claims made previously. The figure shows the change in position of the operating point on the HPC and LPC maps, respectively. The pressure ratio (PR) is on the vertical axis while corrected flow is on the horizontal axis. The blue lines are lines of constant speed and the dashed magenta lines are lines of constant efficiency. The cyan lines are called 'r-lines' and are used in the solution of the operating point position. In terms of HPC operability, it is advantageous to apply power with EM1 and extract power with EM3. Both tend to increase the corrected speed of the HPC while moving the operating point below the operating line and away from the stall line. EM1 is shown to move the operating point further below the operating line with less increase in corrected speed, while the use of EM3 tends to move the operating point more so along the operating line, but noticeably below the operating line. For LPC operability, it is advantageous to apply power with EM1, extract power with EM2, or extract power with EM3. Extracting power with EM3 appears to be the most effective at moving the operating point away from the stall line, followed by injecting power with EM1, and then extracting power with EM2. The application to TEEM will be explored further in Sub-section B.

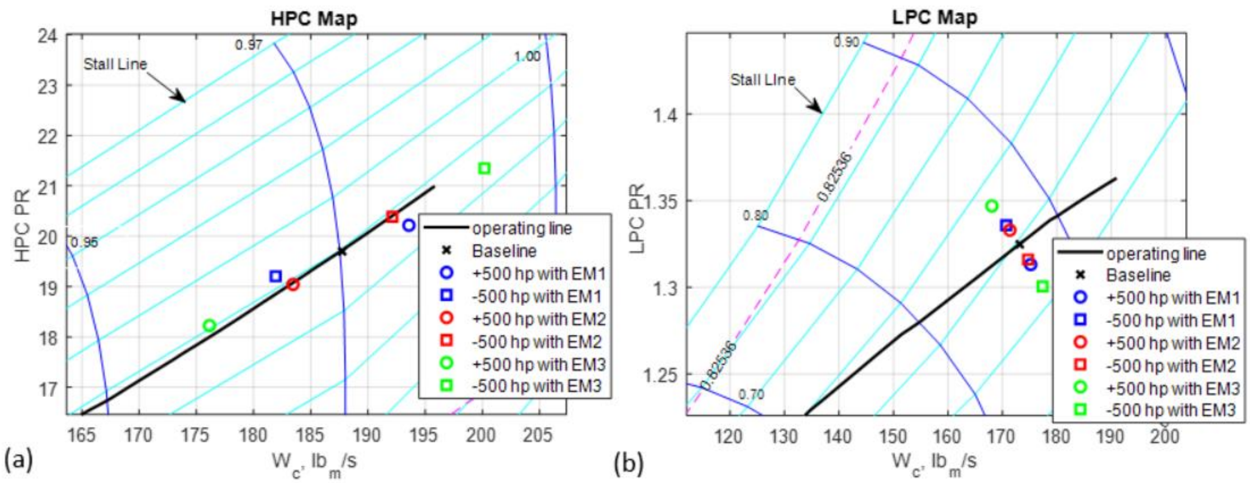


**Figure 12. HPC (a) and LPC (b) performance maps showing the general effects of adding and extracting power.**

Another observation from Fig. 12 is that power injection/extraction with each EM shifts the operating point in different directions. This is illustrated with the blue, red, and green trend lines on the HPC map in Fig. 13. It is also evident by observing the opposing impacts of power extraction and injection of the various EMs in Fig. 12. Theoretically, the EMs could apply or extract power in a variety of combinations to achieve the same operating line on the HPC map. This leads to the hypothesis that the VEATE gearbox could be used to achieve similar performance, operability, and power extraction/injection goals in a variety of ways. Thus, it introduces flexibility to power injection and extraction implementation. Since the use of EM3 shifts power between the spools, it can be used to make more power available on one of the spools for the purpose of extracting it. For example, extracting power with EM3 shifts power to the HPS, which improves the HPC operability. This provides an opportunity to extract more power from the HPS while still maintaining adequate operability margins. A hypothetical example is illustrated in Fig. 13 with the dashed black line and arrows in which the original operating line is maintained while extracting power with EM3 and EM1. The application of power extraction will be further explored in Sub-section C.

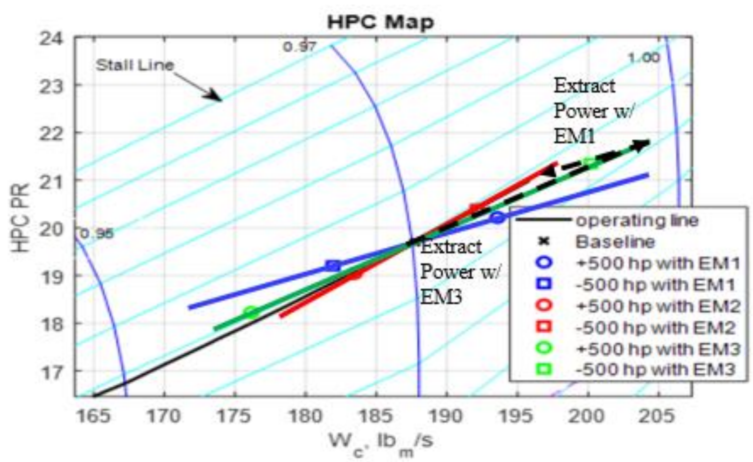


**Figure 13. HPC map with indicated trend directions**

Considering failures of the electric machines, the ability to leverage multiple EMs in the system in order to accomplish the same goal introduces redundancy to the system. For instance, it was hypothesized how EM3 could be used in place of EM1 to address acceleration transients in the application of TEEM. In an application where TEEM and large-scale power extraction are applied together, it is likely that both EM2 and EM3 will be present due to the utility that they both have for power extraction. This will be demonstrated in Sub-section C. In such a case where EM2 and EM3 both exist in the system then EM3 can serve as a backup for EM2 or vice versa to perform TEEM duties. Considering power extraction, if the VEATE gearbox can enable a more even power split between the EMs, it would reduce the severity of a worst-case EM failure.

## B. TEEM Study

In this study, high level control strategies are developed and tested for implementing TEEM during transients based on observations obtained in Sub-section A. Please note that the control approach is not seeking an optimal solution. Rather, it is intended to identify and or confirm potential benefits. Based on the observation in Sub-section A, EM3 is used in place of EM2. The overall control approach is very similar to that applied for the DEM approach, with the exception of using EM3 in place of the LPS EM. EM1 (similar to the HPS EM in the DEM approach) utilizes a HPS speed ($N_{hps}$) controller, and it can also utilize a LPC PR (PR) controller in failure scenarios. The set-points are functions of the commanded fuel flow rate. EM3 can be controlled based on HPC PR or LPC PR. In either case, the set-point commands are scheduled based on the commanded fuel flow rate. The HPC PR controller is utilized during accelerations and the LPC PR controller is utilized during deceleration. EM1 is commanded to apply excess power that is extracted with EM3 during decelerations. For the purpose of demonstration, all the active controllers are Proportional Integral (PI) controllers with integral wind-up protection. In these simulations, EM3 is capable of applying or extracting 200 hp. For comparison purposes, the LPS EM in the DEM approach is of the same power capability. EM1 for the VEATE gearbox approach and the HPS EM for the DEM approach are the same size with a maximum power capability of 400 hp.

A chop and burst transient throttle profile is applied. The engine starts out at full power, then the throttle is moved rapidly to the idle position over the course of 1 second starting at 20 s. It is later moved rapidly back to the full power position over the course of 1 second starting at 55 s. Figure 14 shows the power applied by EM1 and EM3 and the total power required from the ESDs. The power inputs are also shown for the DEM approach. Figure 15 compares the HPC SM and LPC SM of the VEATE gearbox approach with the baseline and DEM approaches. Figure 16 shows the movement of the operating point on the HPC and LPC maps for each of the approaches. As predicted, there is evidence to suggest that extracting power from the ring gear with EM3 is more effective at improving LPC operability during decelerations than directly extracting power from the LPS. This is supported by the elevated LPC stall margin during the deceleration transient as seen in Fig. 15 and the shifting of the operating line on the LPC map in Fig. 16b. The data indicates that EM3 provided superior operability benefits with less control effort. Figure 14 indicates EM3 extracted ~175 hp at its peak power while the LPS EM remained saturated at 200 hp for a significant part of the transient. There is also evidence that the use of EM3 during the acceleration transient boosted the HPC operability improvement. This is illustrated by the elevated HPC stall margin in Fig. 15 during the transient and the further flattening of the HPC operating line in Fig. 16a. In this example, both approaches were observed to increase the minimum HPC stall margin by ~4% and the minimum LPC stall margin by ~1.1%. Another noteworthy result is that use of EM3 during acceleration transients led to an overall lower peak power demand from the ESDs and a significantly lower energy usage. Figure 14 shows that the maximum power was reduced for the VEATE gearbox approach (dotted black line)

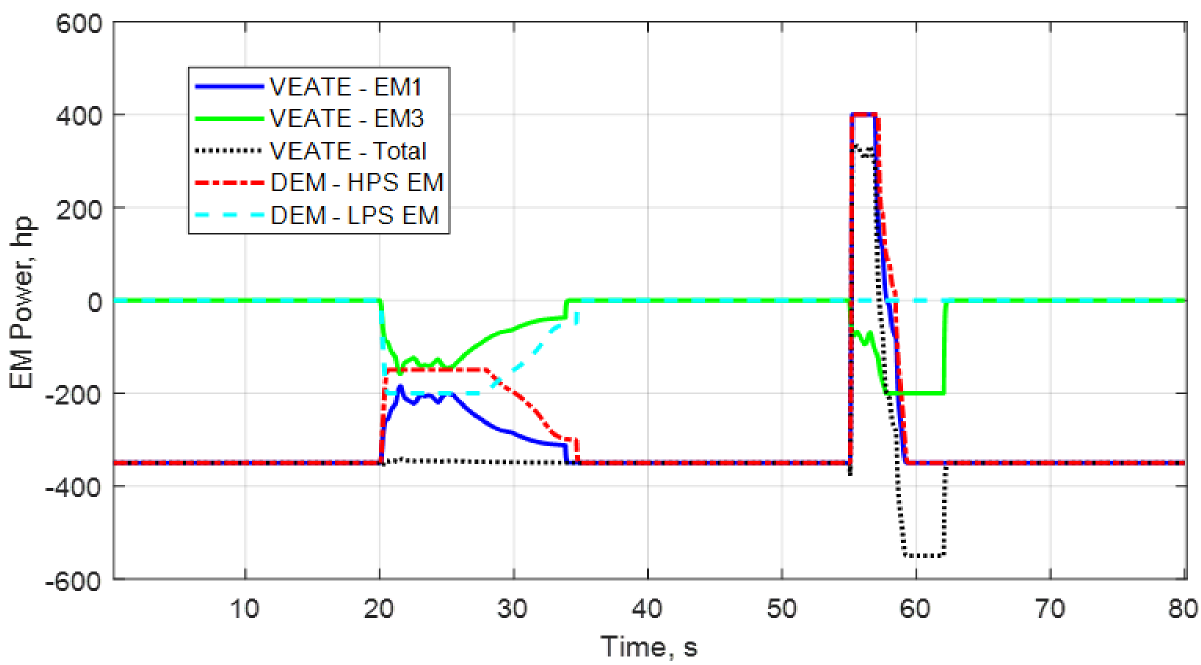


**Figure 14. Power inputs for nominal application of TEEM**

compared to the DEM approach (dashed red line). The maximum power and overall energy usage for the DEM and VEATE gearbox approaches were 400 hp and 0.46 kW-hr, and 330 hp and 0.18 kW-hr, respectively.

In an attempt to quantify the size difference between the LPS EM with the DEM approach and the EM3 for the VEATE gearbox approach, the size of EM3 was reduced until they both achieved similar LPC stall margin responses during the deceleration transient. It was found that EM3 could be reduced to a power level of about 100 hp, making it half the size of the LPS EM.

The VEATE gearbox system could be more advantageous if the application were modified. For example, consider if the power requirements for the acceleration transient were higher, the nominal power extraction from the HPS were lower, and/or a dedicated alternator in the engine's AGB were responsible for the nominal power extraction rather EM1 or the HPS EM. This may lead to the size of these machines being driven by the TEEM application requirements, rather than the nominal power extraction requirement. In this case, the ability to leverage EM3 to aid EM1 during transients would permit EM1 to be smaller and lighter. To illustrate this hypothetical situation, the model was simulated through an acceleration transient with the power injection from EM1 and the HPS EM limited to 250 hp. The power inputs and stall margin results are shown in Fig. 17. It can be observed that the minimum HPC stall margin is improved by ~1.5%, which indicates a need to apply more power with EM1 to get the same HPC stall margin with the DEM approach. Using the HPC SM as the basis for comparison, it was found that the HPS EM power

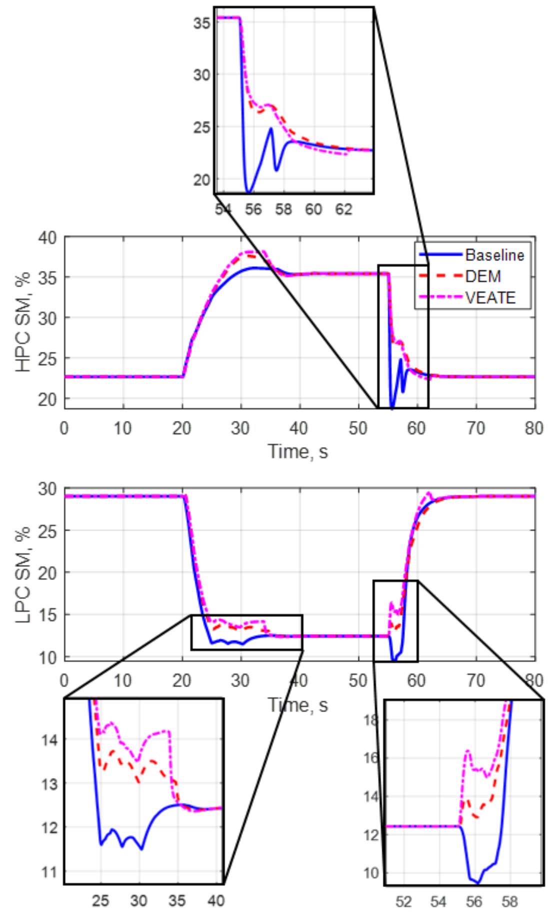


**Figure 15. Stall margin responses with TEEM**

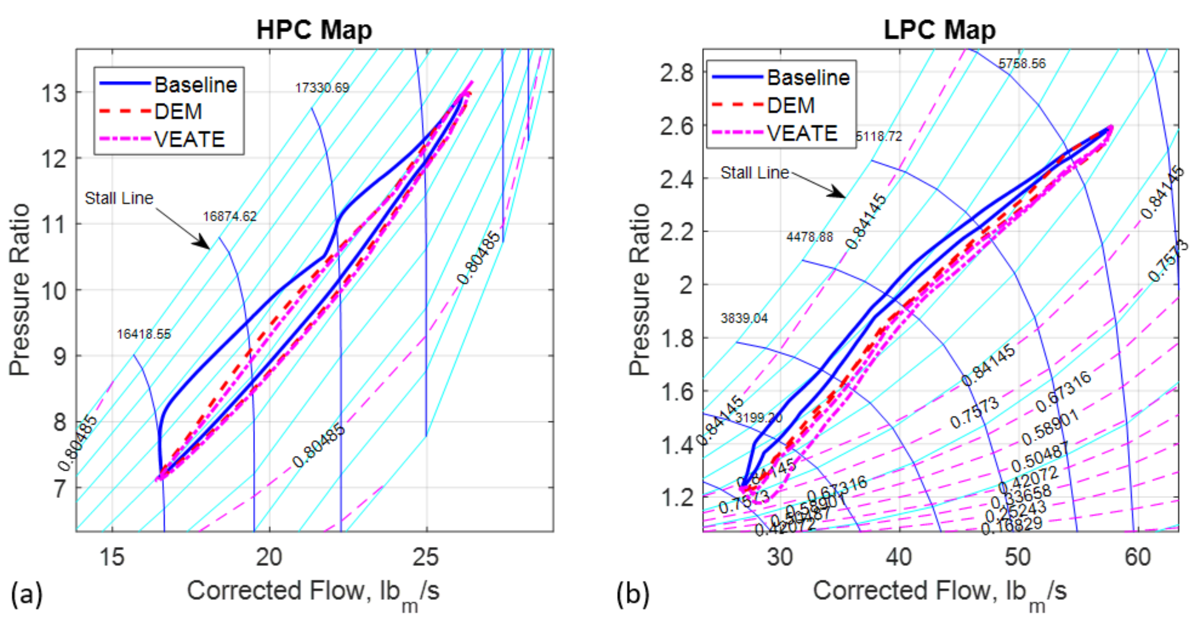


**Figure 16. HPC and LPC performance maps with transient operating lines**

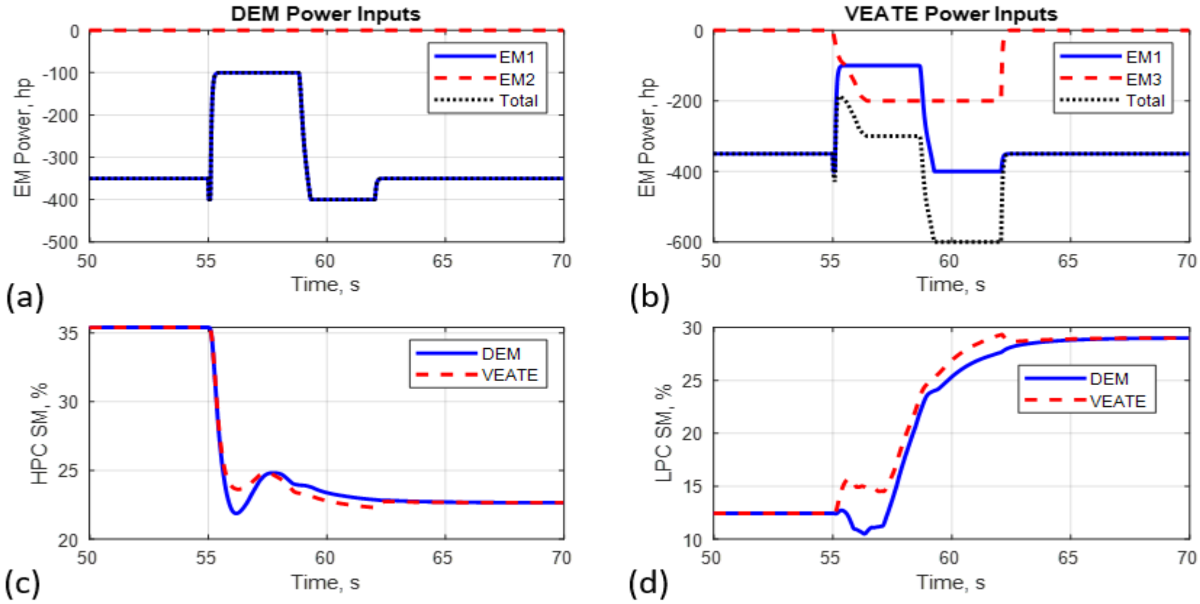


**Figure 17. Power inputs and stall margin response with an imposed EM1 power limit of 250 hp above the nominal power extraction value**

injection during the acceleration transient would need to be increased by ~75 hp to maintain the same minimum HPC SM that was achieved with the help of EM3.

It was hypothesized that the VEATE gearbox approach could enhance the operation of the engine in the event of a failure of EM1. The first concern is a loss of 350 hp of nominal power extraction that helps to power the aircraft

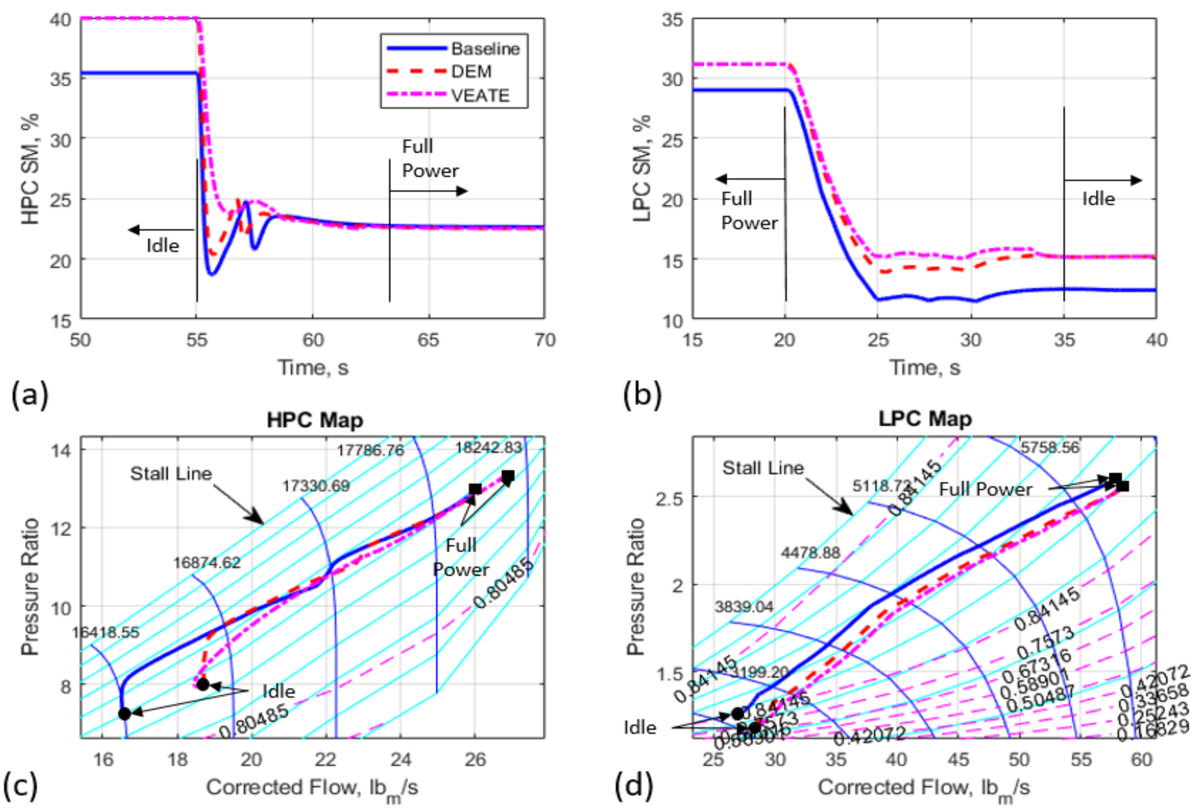


**Figure 18. Operability impact with a failure of EM1 using reversionary control**

systems. The second concern is the loss in ability to use EM1 during transients to improve operability. While there are options for using the remaining EM(s) in the system to help meet the aircraft system power demand, it was assumed that an auxiliary power unit (APU) is present to meet the power demand. Therefore, the engine operates with no nominal power extraction. EM3 is controlled as it normally would be, but without the help of EM1. To provide a reference for comparison, the DEM approach considers a failure of its HPS EM. Like the VEATE gearbox approach, an APU is assumed to be present to meet the aircraft system power demand. The LPS EM is not effective at improving HPC operability and so the loss of the HPS EM will remove the transient operability benefits promised by TEEM for acceleration transients. The LPS EM may be utilized during deceleration transients as it normally would, but without the help of the HPS EM. Figure 18a and 18b presents the HPC stall margin and LPC stall margin results for both approaches. Figure 18c shows the movement of the operating point on the HPC map during the acceleration and Fig. 18d shows the movement of the operating point on the LPC map during the deceleration. Note that the power limit for EM3 was 100 hp for these simulations. The improved stall margin and suppression of the dynamic operating line away from the stall line during the transient relative to the DEM approach demonstrates that the VEATE gearbox approach is superior at retaining operability improvements and is able to do so with less control effort.

### C. Power Extraction Study

In this study, the power extraction is split between EM1, EM2, and EM3 with all of the clutches engaged. Several simulations were conducted with different power splits between the 3 EMs. For each power split, the engine power was increased until an operability limit was encountered or the operating point on a component map hit the edge of the defined performance range. The operability limits considered include stall margin limits, maximum inter-turbine temperature, maximum HPC discharge pressure, maximum LPS speed, and maximum HPS speed. Figure 19a - 19l shows the fraction of the thrust retained at different power splits compared to the maximum thrust target. A color gradient is used to represent the thrust fraction. A value of 1 indicates that the maximum thrust target is achieved. To accommodate the power extraction, the maximum thrust target of the engine was reduced ~17% to ~26,500 $lb_f$. Otherwise the power extraction would be limited by engine operating limits such as turbine inlet temperature. The solid black line in the plots indicates the power splits at which maximum thrust is achieved for a given amount of power extraction. The dashed black line indicates a chosen maximum power extraction goal of 3400 hp (in addition to the 350 hp demand of the aircraft systems). For the purpose of this discussion, the optimal power split occurs at the intersection of the power extraction goal and the maximum thrust line. In other words, the optimal power split will result in the maximum thrust for the given power exaction goal. Each plot (a) – (l) represents and increasing amount of power extraction with EM3 starting at a power fraction (PEx frac) of 0 (or 0%) and working its way to 1 (or 100%). The horizontal axis is the total amount of power extraction, and the vertical axis is the fractional power split between EM1 and EM2 (i.e. the power extraction with EM1 divided by the remainder of power that is not extracted with EM3). Each location in the plots represents a unique power split between EM1, EM2, and EM3. From the figures, it is evident that extracting more power with EM3 favors more power extraction from EM1 and less from EM2. This can be seen by the shifting of the thrust metrics up on the plots as more power is extracted with EM3. Thus, one can see that the impact of extracting power with EM3 is to shift the optimal power split, creating a continuum of power split options that achieve similar thrust and power extraction metrics. This effect is explained by the results observed in study presented in Sub-section A. The use of EM3 is influencing power transfer from the LPS to the HPS, which makes more power available for power extraction on the HPS and less available on the LPS. Thus, it is possible to extract the same amount of total power, remove essentially the same amount of power from each spool, and achieve essentially the same engine performance, but have different power splits with the electric machines.

As suggested previously, a potential benefit is flexibility in the power system design which may occur independent of the turbomachinery design. In this instance, the maximum power extraction demand without the VEATE gearbox system would call for ~15% of the power needed to drive the hypothetical electrically driven propulsors to be extracted from the HPS and the remaining ~85% to come from the LPS. This is based on Fig. 19a, using the intersection of the power extraction goal and maximum thrust line as guidance for the selection. This would indicate the need to integrate a very large EM or a number of EMs with the LPS, which could introduce integration challenges. The VEATE gearbox approach provides flexibility in the choice of power splits, thus allowing the EMs to be sized such that it facilitates easier integration. For example, in this application EM1/EM2/EM3 power splits of 32%/48%/20% (based on Fig. 19e) or 55%/0%/45% (based on Fig. 19j) could be advantageous. Both cases have more even power splits, which will also reduce the worst-case loss of power extraction capability in the event of EM failures. The latter option can achieve similar performance and operability without an EM coupled directly to the LPS. This architecture also matches the architecture proposed previously for the TEEM application.

With a power split of 32%/48%/20%, the overall power extraction capability for a failure of each EM is presented in Fig. 20. Figure 20 also presents the similar information for the DEM approach for failure situations of each of its

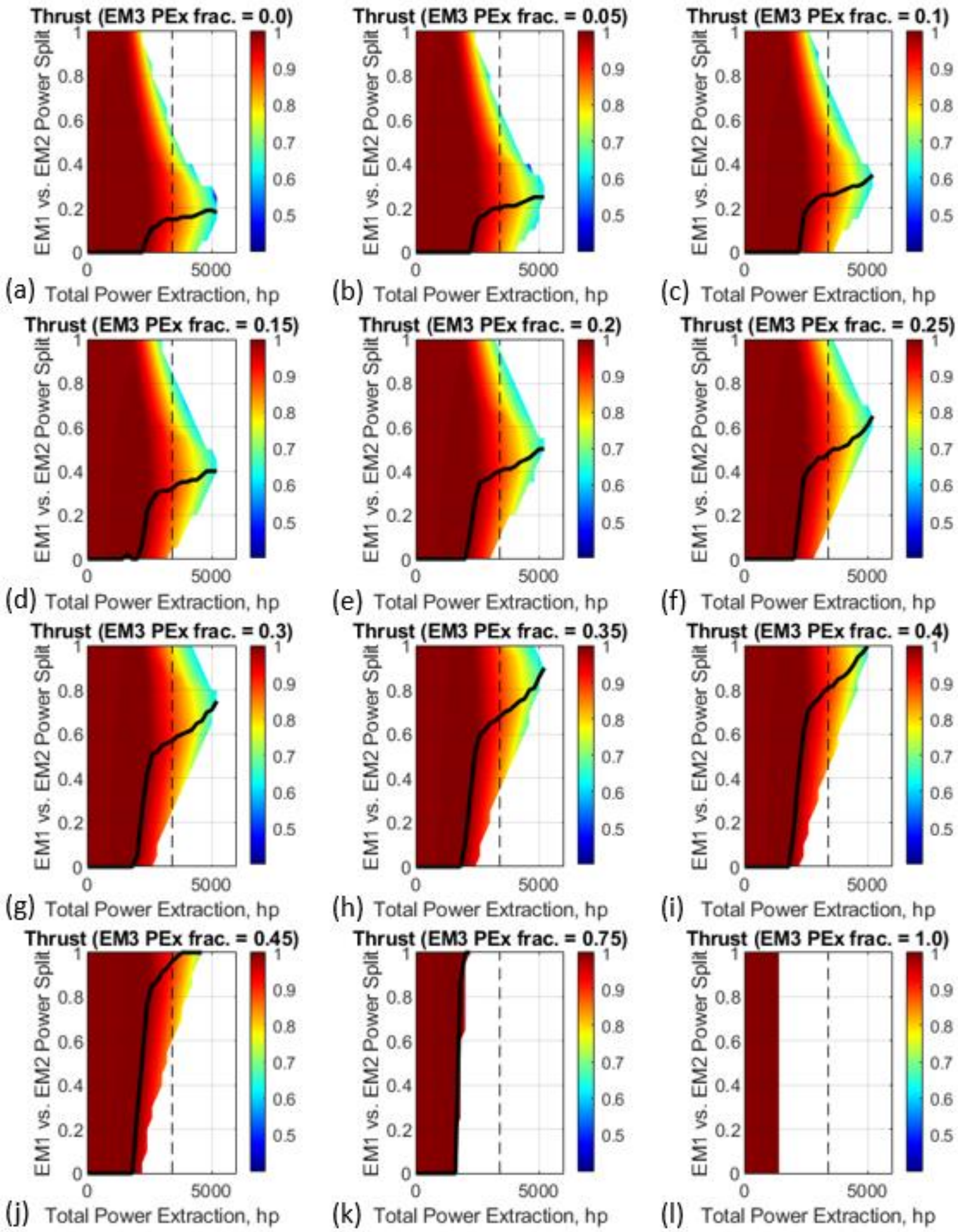


**Figure 19. Thrust variation with power extraction and power splits**

EMs. It is evident that a worst-case failure of the VEATE gearbox approach retains much more capability than the DEM approach. In fact, the DEM approach would be unable to meet the idle power extraction goal under full power conditions whereas the VEATE gearbox approach would be able to retain over half of the power extraction request for the propulsion system.

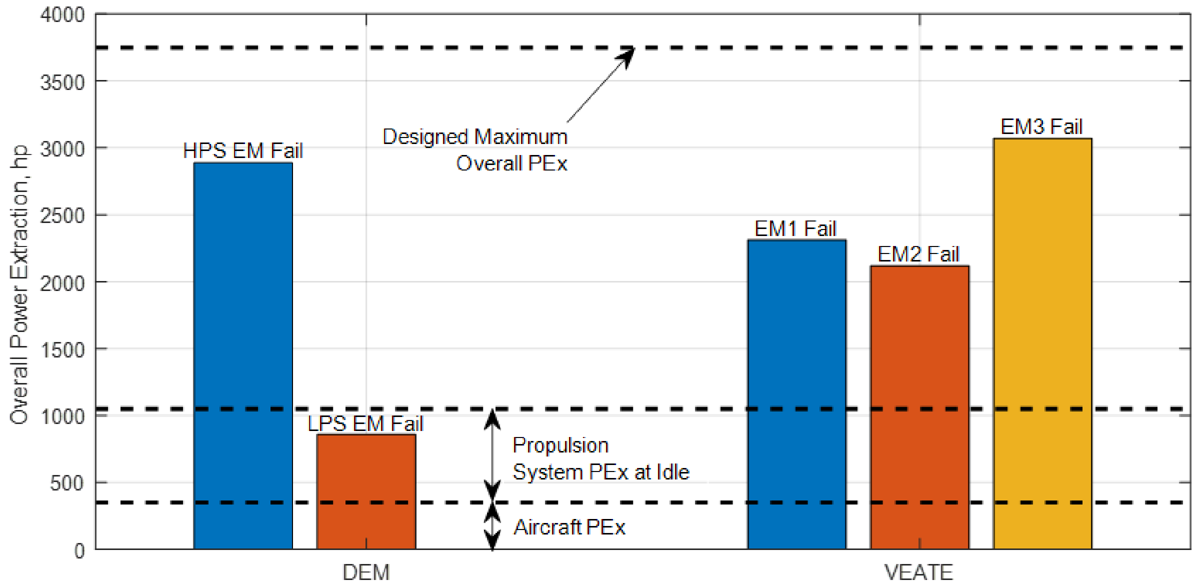


**Figure 20. Maximum power extraction capability with EM failures**

## VII. Mass Analysis

A mass approximation of the VEATE gearbox system was made using a regression analysis for aerospace power transmission gear boxes. The models used to approximate the mass are given by Eq. (9) and (10).

$$M = 0.176\tau^{0.824} \tag{9}$$

$$M = 0.109\tau^{0.824} \tag{10}$$

In these equations, $M$ is the mass of the gearbox or gearbox sub-component (including support systems for lubrication, etc.) in $lb_m$ and $\tau$ is the maximum torque in units of ft-$lb_f$ observed in that gearbox or gearbox sub-component. Eq. (9) was used to approximate the mass of the planetary gearbox with multiple power flow paths and Eq. (10) was used to approximate the mass of the components with a single power flow path (e.g. the gearing between the HPS and HPS sun gear, and the gearing of the EMs for the DEM approach). The equations were derived from data used in the derivation of a commonly used correlation that relates gearbox mass to torque, and speed ratio [16]. The data set consists of single main rotor helicopter gearboxes and engine gearboxes. Data for tandem rotor and tilt rotor data was added. In particular, these gearboxes were used to create Eq. (9) because these gearboxes have multiple outputs and resemble the planetary gearboxes of the VEATE gearbox better than the single rotor gearboxes. They are also heavier and thus provide a more conservative mass estimate. Eq. (10) utilized the data for the single rotor helicopter gearboxes, and engine gearboxes. The new equations relate the gearbox mass only to the torque. Figure 21 shows the

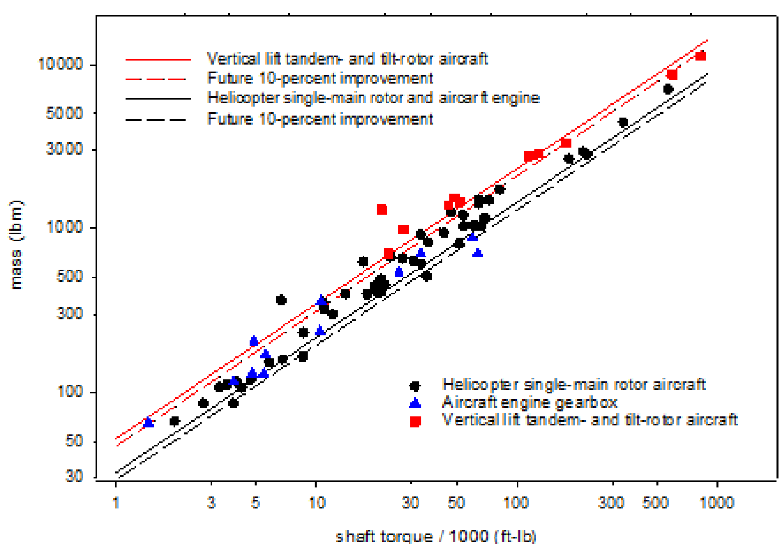


**Figure 21. Gearbox mass data with recommended trend lines**

data and the fit. The root mean square values of the regressions were above 0.965 and the standard errors of the mean were less than 3 $lb_m$. The errors used in the regression analysis utilized the log format of the equations.

$$log(M) = log(K) + Clog(\tau) \tag{11}$$

Note that K and C are constants. Thus, the errors were based on the values of *log(M)*. The gearbox masses were approximated based on data from the simulations. The gearbox masses are listed in Table 2.

It may be possible to reduce the size of the power system. For the strict application of the TEEM transient operability concept, EM3 requires less power to improve operability during decelerations than does an EM connected to the LPS. In addition, the other EMs in the system, can be leveraged during accelerations to assist EM1, showing the potential to reduce the size of EM1 and it supporting equipment. However, for the AGTF30 engine application, EM1 (and the HPS EM for the DEM approach) is sized based on nominal power extraction requirements that happened to be sufficient for implementing TEEM. Therefore, a benefit in reducing the size of EM1 cannot be demonstrated. However, it is possible to reduce the size of the power system required for decelerations in this application. It was observed that a 100hp EM3 was capable of providing the same operability in terms of stall margin during decelerations as a 200hp EM2. Ref. [17], suggests a power density of 9.9 kV-A/kg for both the motor and the inverter/rectifier. Ignoring details such as cable mass, the study results suggest that the power system mass could be reduced by more than 33 $lb_m$ strictly by using EM3 as opposed to using the LPS EM with a DEM approach. In addition, a reduction in energy usage was demonstrated when EM3 was used during accelerations, which would contribute to the reduction in mass of the energy storage system and an overall reduction in the mass of the power system. One could expect that less power and energy requirements would result in compounded mass reductions elsewhere in the system. However, that analysis is beyond the scope of this preliminary evaluation.

Based on the approximations of gearbox mass and a conservative estimate of power system mass reduction, the VEATE gearbox would more than offset the projected mass of the gearbox for the TEEM only application and, at minimum, offset the additional mass of the gearbox as compared to the DEM approach.

**Table 2. Gearbox mass approximations**

| TEEM implementation | | Power Extraction with TEEM | |
|---|---|---|---|
| DEM | VEATE | DEM | VEATE |
| 29.6 $lb_m$ | 35.0 $lb_m$ | 96.7 $lb_m$ | 126.3 $lb_m$ |

## VIII. Conclusion

The Versatile Electrically Augmented Turbine Engine (VEATE) gearbox, described herein, provides a hybrid method for managing power on the spools of a gas turbine engine while interfacing electric machines (EMs) with turbomachinery. Such a system offers flexibility in how to manage power in an electrified gas turbine engine. A dynamic model for the system has been presented and demonstrated to study the potential benefits of the system. The physical characteristics of the VEATE gearbox were not optimized, but benefits were still able to be presented. Based on the results, there is evidence to suggest that the VEATE gearbox system has the potential to reduce power system size, particularly for the application of Turbine Electrified Energy Management (TEEM) for transient operability control. It also introduces flexibility for power extraction implementation, and it improves safety through inherent fail-safe features that include redundancy. In particular, it enables more even power splits that result in better worst-case EM failure modes with application to power extraction, and it provides backup options for implementing TEEM that introduces redundancy. Weight approximations project a modest weight benefit over the DEM approach. Overall, the VEATE concept appears to have utility that encourages further investigation.

## Appendix A

This appendix includes the dynamic equations that govern the motion for each of the components of the DP gearbox. This includes variants of the equations that result from different clutch configurations. At the end of the appendix, the iterative process for determining the correct clutch lock configuration is described.

<u>HPS</u>

$$J_{hps}\dot{\omega}_{hps} = \eta_{hps}\left(\tau_{hps} + r_{hps}f_{hps}\right) \tag{12}$$

Speed reduction shaft

$$J_{red}\dot{\omega}_{red} = \eta_{red}\left(r_{red1}f_{hps} + r_{red2}f_{red}\right) \tag{13}$$

Sun gear

*Independent:*

$$J_s\dot{\omega}_s = \eta_s\left(r_{reds}f_{red} - n_p r_s f_{sp} + \tau_{CA}\right) \tag{14}$$

*Clutch A locked:*

$$(J_s + J_{em1})\dot{\omega}_{s/em1} = \eta_s\left(r_{reds}f_{red} - n_p r_s f_{sp}\right) + \eta_{em1}\tau_{em1} \tag{15}$$

Planets

$$J_p\dot{\omega}_p = \eta_p r_p\left(f_{pr} - f_{sp}\right) \tag{16}$$

$$m_p\left(r_s + r_p\right)\dot{\omega}_{lps} = f_{sp} + f_{pr} - f_{pc} \tag{17}$$

Carrier (LPS)

$$J_{lps}\dot{\omega}_{lps} = \eta_{lps}\left[\tau_{lps} + n_p\left(r_s + r_p\right)f_{pc} + r_{cg}f_{em2}\right] \tag{18}$$

Ring gear

$$J_r\dot{\omega}_r = \eta_r\left(r_{rg}f_{em3} - n_p r_r f_{pr}\right) \tag{19}$$

EM1

*Independent:*

$$J_{em1}\dot{\omega}_{em1} = \eta_{em1}(\tau_{em1} - \tau_{CA}) \tag{20}$$

*Clutch A locked:*

*Same as Eq. (*15*)*

EM2

*Independent:*

$$J_{em2}\dot{\omega}_{em2} = \eta_{em2}(\tau_{em2} - \tau_{CB}) \tag{21}$$

*Clutch B locked:*

$$\left(J_{em2} + J_{em2g}\right)\dot{\omega}_{em2/em2g} = \eta_{em2}\tau_{em2} + \eta_{em2g}r_{em2g}f_{em2} \tag{22}$$

EM3

*Independent:*

$$J_{em3}\dot{\omega}_{em3} = \eta_{em3}(\tau_{em3} - \tau_{CC}) \tag{23}$$

*Clutch C locked:*

$$\left(J_{em3} + J_{em3g}\right)\dot{\omega}_{em3/em3g} = \eta_{em3}\tau_{em3} + \eta_{em3g}r_{em3g}f_{em3} \tag{24}$$

EM2 Gear

*Independent:*

$$J_{em2g}\dot{\omega}_{em2g} = \eta_{em2g}\left(\tau_{CB} + r_{em2g}f_{em2}\right) \tag{25}$$

*Clutch B locked:*

*Same as Eq. (22)*

EM3 Gear
*Independent*

$$J_{em3g}\dot{\omega}_{em3g} = \eta_{em3g}(\tau_{CC} + r_{em3g}f_{em3}) \tag{26}$$

*Clutch C locked:*

$$Same\ as\ Eq.\ (24)$$

The clutch lock configuration is determined using the iterative process outlined below:

(1) The clutch lock configuration and clutch torques are initialized. If the clutch is disengaged, the clutch torque is zero and the lock status is unlocked. If the clutch is engaged but not locked, then it is slipping. In this case, the lock status is unlocked and the clutch torque is evaluated using the following equation which is expressed generically so that it is applicable to each clutch.

$$\tau_C = \frac{2}{3}R_C X_C \mu_{kC} sign(N_a - N_b) \tag{27}$$

$N_a$ and $N_b$ refer to the speeds of the components on each side of the clutch. If the clutch is commanded to engage and the error in speed between the 2 rotating parts is below the acceptable threshold value, then the lock status is changed to locked and the clutch torque is initialized at zero. If the clutch was locked during the previous iteration and it is still commanded to be engaged, then the lock status remains locked and the clutch torque is initialized with its prior value.

(2) The linear system of equations is solved with the initial clutch lock configuration and clutch torques. This solution only utilizes Eq. (1) – (7).

(3) The solution from (2) is used to determine if a speed crossing will occur within the time step for any clutch that is engaged but slipping. If a speed crossing is predicted, then the clutch torque required to achieve the speed match is calculated through another solution of the system of equations that includes the relevant clutch torques as unknowns. The calculated clutch torque is modified by what is being called a convergence factor. This factor has a value between 0 and 1. While it is not a physically real quantity, it promotes a smoother and more predictable transition to a locked clutch state.

(4) If the clutch is locked then the clutch torque is computed using an expression derived from $\dot{\omega}_a = \dot{\omega}_b$ where the subscripts "$a$" and "b" refer to the rotating part of one each side of the clutch. Substituting the appropriate expressions from Appendix A and using values of the forces calculated from the previous solution of the system of equations enables the explicit calculation of the desired locked clutch torques.

(5) The clutch torques are compared with the maximum static friction torque limit. If the magnitude of the clutch torque exceeds this torque then the lock status is set to unlocked and Eq. (27) is used to calculate the torque. The static friction torque limit is calculated with Eq. (28).

$$\tau_C = \frac{2}{3}R_C X_C \mu_{sC} \tag{28}$$

(6) The system of equations is solved using the appropriate expressions from Appendix A, which should be consistent with the latest clutch lock configuration and use the latest clutch torque values. This solution only utilizes Eq. (1) – (7).

(7) Repeat steps 1-6 at least once more until the clutch lock configuration from the current iteration matches the clutch lock configuration from the previous iteration.

## Appendix B

This appendix quantifies each of the parameters used in the VEATE gearbox model. Note that the inertia of the EMs changes based on their maximum power.

**Table 3. General and miscellaneous parameters**

| | |
|---|---|
| $n_p$ | 4 |
| $m_p$ | 2.78 $lb_m$ |
| Maximum number of iterations | 50 |
| Convergence parameter | 0.8 |
| Simulation time-step | 0.015 s |

**Table 4. Gear radii**

| | |
|---|---|
| $r_{hps}$ | 1.5 in |
| $r_s$ | 2 in |
| $r_r$ | 5.5 in |
| $r_p$ | 1.75 in |
| $r_{red1}$ | 2.25 in |
| $r_{red2}$ | 1.5 in |
| $r_{reds}$ | 2.25 in |
| $r_{cg}$ | 2 in |
| $r_{rg}$ | 2.25 in |
| $r_{em2g}$ | 2 in |
| $r_{em3g}$ | 2.25 in |

**Table 5. Component inertias**

| | |
|---|---|
| $J_{hps}$ | 1.86 slug-ft$^2$ |
| $J_{lps}$ (includes the reflected inertia of the fan) | 7.34 slug-ft$^2$ |
| $J_s$ | 0.0041 slug-ft$^2$ |
| $J_p$ | 0.00092 slug-ft$^2$ |
| $J_r$ | 0.037 slug-ft$^2$ |
| $J_{red}$ | 0.0030 slug-ft$^2$ |
| $J_{em1}$ | (0.0015 x EM power level in hp) slug-ft$^2$ |
| $J_{em2}$ | (0.0015 x EM power level in hp) slug-ft$^2$ |
| $J_{em3}$ | (0.0015 x EM power level in hp) slug-ft$^2$ |
| $J_{em2g}$ | 0.004 slug-ft$^2$ |
| $J_{em3g}$ | 0.004 slug-ft$^2$ |

**Table 6. Clutches**

| | |
|---|---|
| $R_{CA}$ | 1.8 in |
| $X_{CA}$ | 250 lb$_f$ |
| $\mu_{kCA}$ | 0.5 |
| $\mu_{sCA}$ | 1000 |
| $R_{CB}$ | 1.8 in |
| $X_{CB}$ | 250 lb$_f$ |
| $\mu_{kCB}$ | 0.5 |
| $\mu_{sCB}$ | 1000 |
| $R_{CC}$ | 3 in |
| $X_{CC}$ | 250 lb$_f$ |
| $\mu_{kCC}$ | 0.5 |
| $\mu_{sCC}$ | 1000 |
| *Maximum acceptable speed matching error* | 5 rpm |

**Table 7. Efficiencies**

| | |
|---|---|
| $\eta_{hps}$ | 1.0 |
| $\eta_{lps}$ | 1.0 |
| $\eta_s$ | 0.99 |
| $\eta_p$ | 0.99 |
| $\eta_c$ | 0.99 |
| $\eta_r$ | 0.99 |
| $\eta_{red}$ | 0.995 |
| $\eta_{em1}$ | 0.998 |
| $\eta_{em2}$ | 0.998 |
| $\eta_{em3}$ | 0.998 |
| $\eta_{em2g}$ | 0.998 |

| | |
|---|---|
| $\eta_{em3g}$ | 0.998 |

**Acknowledgments**

The authors would like to acknowledge the Transformational Tools & Technologies (TTT) project under the NASA Aeronautics Research Mission Directorate (ARMD) that has supported this work. The authors would also like to acknowledge Tim Krantz at the NASA Glenn Research Center for providing some general consulting and providing the model used to approximate the gearbox weight.

## References

[1] Jansen, J. H., Bowman, C., Jankovsky, A., Dyson, R., Felder, J., "Overview of NASA Electrified Aircraft Propulsion Research for Large Subsonic Transports," AIAA 2017-4701, AIAA Propulsion and Energy Forum, Atlanta, GA. 2017. (NASA NTRS Document ID: 20180000361)

[2] Johnson, W., Silva, C., and Solis, E., "Concept Vehicles for VTOL Air Taxi Operations," American Helicopter Society Conference of Aeromechanics Design for Transformative Vertical Flight, Alexandria, VA. 2018. (NASA NTRS Document ID: 20180003381)

[3] Welstead, J. R., Felder, J. L., "Conceptual Design of a Single-Aisle Turboelectric Commercial Transport with Fuselage Boundary Layer Ingestion," AIAA 2016-1027, AIAA SciTech Forum, San Diego, CA. 2016. (NASA NTRS Document ID: 20160007674)

[4] Felder, J. L., Tong, M. T., Chu, J., "Sensitivity of Mission Energy Consumption to Turboelectric Distributed Propulsion Design Assumptions on the N3-X Hybrid Wing Body Aircraft," AIAA 2012-2701, 48th AIAA/ASME/SAE/ASEE Joint Propulsion Conference & Exhibit, Atlanta, GA. 2012. (NASA NTRS Document ID: 20130010734)

[5] Chapman, J., "A Study of Large Scale Power Extraction and Insertion on Turbofan Performance and Stability," AIAA 2020-3547, AIAA Propulsion & Energy Forum, 2020. (NASA NTRS Document ID: 20205004868)

[6] Culley, D., Kratz, J., and Thomas, G., "Turbine Electrified Energy Management (TEEM) For Enabling More Efficient Engine Designs," AIAA 2018-4798, AIAA Propulsion & Energy Forum, Cincinnati, OH. 2018. (NASA NTRS Document ID: 20190002775)

[7] Kratz, J., Culley, D., Thomas, G., "A Control Strategy for Turbine Electrified Energy Management," AIAA 2019-4499, AIAA Propulsion & Energy Forum, Indianapolis, IN. 2019. (NASA NTRS Document ID: 20190032490)

[8] Kratz, J., Culley, D., and Thomas, G., "Evaluation of Electrical System Requirements for Implementing Turbine Electrified Energy Management," AIAA 2019-4502, AIAA Propulsion & Energy Forum, Indianapolis, IN, 2019. (NASA NTRA Document ID: 20190030360)

[9] Philpot, M., "Practical Consideration In Designing the Engine Cycle," Defense Technical Information Center, 1992.

[10] Stevens, M., Lewicki, D., and Handschuh, R., "Concepts for Multi-Speed Rotorcraft Drive Systems – Status of Design and Testing at NASA GRC," American Helicopter Society Annual Forum, Virginia Beach, VA. 2015. (NASA NTRS Document ID: 20150010716)

[11] Jones, S. M., Haller, W. J., Tong, M. T., "An N+3 Technology Level Reference Propulsion System," NASA/TM-219501. 2017.

[12] Chapman, J., Lavelle, T., May, R., Litt, J., and Guo, T.-H., "Toolbox for the Modeling and Analysis of Thermodynamic Systems (T-MATS) User's Guide," NASA TM-2014-216638, 2014.

[13] Claus, R.W., Evans, A.L., Lylte, J.K. and Nichols, L.D., "Numerical Propulsion System Simulation," Computing Systems in Engineering, Vol 2, No. 4, pp 357-364, 1991.

[14] Chapman, J., and Litt, J., "Control Design for and Advanced Geared Turbofan Engine," AIAA 2017-4820, AIAA Propulsion & Energy Forum, Atlanta, GA, 2017. (NASA NTRS Document ID: 20170010711)

[15] Tong, M. T., Naylor, B. A., "An Object-oriented Computer Code for Aircraft Engine Weight Estimation," Proceedings of ASME Turbo Expo 2008, Berlin, Germany. 2008. (NASA NTRS Document ID: 20100000016)

[16] Brown, G., Kascak, A., Ebihara, B., Johnson, D., Choi, B., Siebert, M., and Buccieri, C., "NASA Glenn Research Center Program in High Power Density Motor for Aeropropulsion," NASA/TM-213800. 2005.

[17] Sadey, D., Csank, J., Hanlon, P., and Jansen, R., "A Generalized Power System Architecture Sizing and Analysis Framework," AIAA 2018-4616, AIAA Propulsion & Energy Forum, Cincinnati, OH. 2018. (NASA NTRS Document ID: 20180005332)